Lead Discovery of Dual G-Quadruplex Stabilizers and Poly(ADP-ribose) Polymerases (PARPs) Inhibitors: A New Avenue in Anticancer Treatment

Journal:	*Journal of Medicinal Chemistry*
Manuscript ID	jm-2016-015635.R2
Manuscript Type:	Article
Date Submitted by the Author:	n/a
Complete List of Authors:	Salvati, Erica; Regina Elena National Cancer Institute, Botta, Lorenzo; Columbia University, Chemistry Amato, Jussara; Università degli Studi di Napoli "Federico II", Dipartimento di Chimica delle Sostanze Naturali Di Leva, Francesco; University of Naples "Federico II", Department of Pharmacy Zizza, Pasquale; Regina Elena National Cancer Institute, Gioiello, Antimo; Università degli Studi di Perugia, Laboratory of Medicinal and Advanced Synthetic Chemistry (Lab MASC), Dipartimento di Scienze Farmaceutiche Pagano, Bruno; Università di Napoli "Federico II", Dipartimento di Chimica Farmaceutica e Tossicologica Graziani, Grazia; University of "Tor Vergata", Rome, Italy, Department of Systems Medicine, Tarsounas, Madalena ; University of Oxford, Oxford Institute for Radiation Oncology Randazzo, Antonio; Univ. degli Studi di Napoli Federico II, Department of Pharmacy Novellino, Ettore; University of Naples Federico II, Pharmaceutical and Toxicological Chemistry Biroccio, Annamaria; Regina Elena Cancer Institute, Department of Experimental Chemotherapy Cosconati, Sandro; University of Campania Luigi Vanvitelli, DiSTABiF

Lead Discovery of Dual G-Quadruplex Stabilizers and Poly(ADP-ribose) Polymerases (PARPs) Inhibitors: A New Avenue in Anticancer Treatment

Erica Salvati,[‖£] Lorenzo Botta,[§£] Jussara Amato,[§£] Francesco Saverio Di Leva,[§] Pasquale Zizza,[‖] Antimo Gioiello,[‡] Bruno Pagano,[§] Grazia Graziani,[¥] Madalena Tarsounas,[±] Antonio Randazzo,[§] Ettore Novellino,[§] Annamaria Biroccio[‖] and Sandro Cosconati[†*]*

[‖] Oncogenomic and Epigenetic Unit, Regina Elena National Cancer Institute, 00158 Rome, Italy. [§]Department of Pharmacy, University of Naples "Federico II", 80131 Naples, Italy. [‡]Department of Pharmaceutical Science, University of Perugia, I-06123 Perugia, Italy. [±]Genome Stability and Tumourigenesis Group, CRUK/MRC Oxford Institute for Radiation Oncology, Department of Oncology, University of Oxford, Old Road Campus Research Building, Oxford OX3 7DQ, UK [¥]Department of Systems Medicine, University of "Tor Vergata", Rome, Italy. [†]DiSTABiF, University of Campania Luigi Vanvitelli, 81100 Caserta, Italy.

Abstract

G-quadruplex stabilizers are an established opportunity in anticancer chemotherapy. To circumvent the antiproliferative effects of G4 ligands, cancer cells recruit PARP enzymes at telomeres. Herein, starting from the structural similarity of a potent G4 ligand previously discovered by our group and a congeneric PARP inhibitor, a library of derivatives was synthesized to discover the first dual G4/PARP ligand. We demonstrate that a properly decorated thieno[3,2-c]quinolin-4(5H)-one stabilizes the G4 fold *in vitro* and in cells, induces a DNA damage response localized to telomeres, inhibits PARylation in cells and has an antiproliferative effect in BRCA2 deficient tumor cells.

Introduction.

Telomeres are essential chromosomal components, which warrant the correct replication and safeguard of chromosome termini. These are constituted by TTAGGG repeats with a 2–20 kb long double-stranded DNA and a 50–500 nucleotide long single-stranded region.[1] Parallel to normal cells proliferation, telomeres get progressively shorter causing irreparable growth arrest (cellular senescence).[2] A specialized reverse transcriptase, telomerase, provides a maintenance mechanism that keeps the telomere length constant, despite cell proliferation, through the addition of the copies of the TTAGGG motif at the end of the 3′ single-stranded overhang. The transcription of this enzyme is repressed in almost all differentiated human somatic cells.[3] Interestingly, roughly 85% of tumor cells feature a telomerase overexpression;[4] while, in the remainder 15% of human cancers, telomerase activity is absent and telomere maintenance is achieved by a mechanism that involves recombination events between telomeres, called alternative lengthening of telomere (ALT).[5] Through both the aforementioned mechanisms, telomeres are kept to a constant length with the resulting senescence bypass and immortalization of cells.[6] This unlimited proliferative potential is one of the distinctive hallmarks of cancer.

Thus, it is now well established that telomere maintenance and safeguard have a critical role in carcinogenesis.[7] In this scenario, agents that can influence telomere preservation should have potential implications for anti-cancer therapy. In the last decades, compelling body of evidence outlined that induction of cancer cell senescence and apoptosis can be induced via indirect mechanisms.[8] In particular, it is now well accepted that the 3′ single-stranded overhang of telomeric DNA can adopt the G-quadruplex (G4) fold.[8] In cells, the G4 stabilization by small molecules initially alters the G-overhang structure and triggers the release of shelterin protein POT1 from telomeres,[9] t-loop instability, anaphase bridges and telomere loss associated with

shelterin protein TRF2 release.[10] This mechanism is regarded as "telomere uncapping" and a number of studies now confirm G4 structures as effective targets for anticancer therapy.[11]

Moreover, the pharmacological stabilization of G4 triggers specific recruitment and activation of different protein factors at telomere level such as helicases, Topoisomerase I and IIIα (TOP1 and IIIα) and poly(ADP-ribose) polymerases (PARPs).[12] In this respect, several PARP family proteins can be associated with telomeres such as Tankyrases (TNKS) 1 and 2 as well as PARP1 and 2, where they can poly(ADP-ribosyl)ate TRF1 and TRF2, influencing their association with telomeric DNA and acting as enhancers of its elongation.[12] Moreover, upon DNA damage PARP enzymes have been demonstrated to contribute to telomere protection against end-to-end fusions and genomic instability. The close interplay between G4 stabilization and specific PARP enzyme recruitment and activation has been demonstrated by our group.[12] In particular, upon treatment with a well-characterized G4 ligand (RHPS4), PARPs are recruited at telomeres. Moreover, the concomitant inhibition by PARP inhibitors prevents repairing of DNA breaks induced by G4 stabilization. This eventually leads to increased chromosome abnormalities and inhibition of tumor cell growth both *in vitro* and in tumor xenografts.

This evidence raises a new opportunity for drug intervention through the concomitant G4 stabilization and PARP1 inhibition. Indeed, the development of single agents that have multiple targets has some intrinsic advantages over the use of a combination of single-target drugs.[13] Therefore, considering the synergistic effect on tumor cells of G4 stabilization and PARPs inhibition and the advantage of multiple-target drugs, herein we aimed at finding the first lead compound with a dual G4/PARP mechanism of action. This idea was stimulated by the structural similarities shared by a G4 ligand (compound **1**, Chart 1) discovered by our group in 2013,[14] and a class of potent PARP1 inhibitors reported in the literature (**2**, Chart 1).[15] In particular, while **1**

features a 5,9b-dihydrothieno[3,2-c]quinolin-4(3aH)-one scaffold which is predicted to stack at the 3' of the G4 DNA,[14] **2** features an isoquinolinone-based tricycle which bears the critical groups responsible for PARP binding and inhibition.[15]

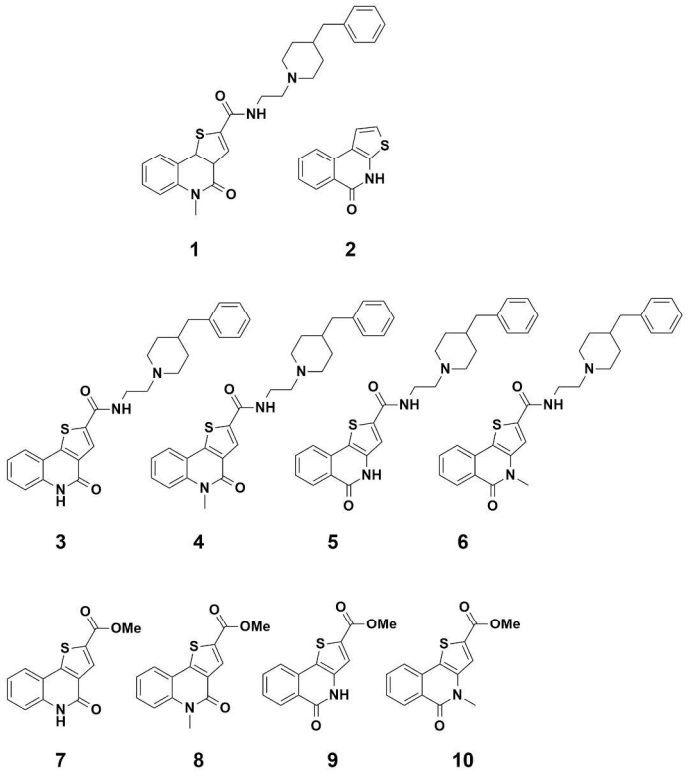

Chart 1. Structures of the lead compounds (**1** and **2**) and the designed analogs (**3**-**6**, **7**-**10**).

Therefore, starting from compounds **1** and **2** we designed and synthesized a small library of four compounds alternatively bearing a thieno[3,2-c]quinolin-4(5H)-one scaffold (compounds **3**, **4, 7,** and **8**) and a thieno[3,2-c]isoquinolin-5(4H)-one one (**5**, **6**, **9**, and **10**). Considering the already published data outlining the effect of the methyl substituent on the quinolinone nitrogen on PARP1,[15] this structure-activity relationship was also explored in our ligands (see **1** and **5** *vs* **4** and **6**). Moreover, to explore the effect of the basic chain, attached to the core scaffold, on both the G4 stabilizing properties and PARP inhibition, we also decided to test the derivatives devoid of this chain (compounds **7**-**10**). The main idea behind the synthesis of compounds **3**-**10** was to

find the best core scaffold that retains sufficient affinity and activity at both targets (namely telomeric G4 DNA and PARP enzymes).

Results and Discussion.

Chemistry. The synthetic pathways followed for the preparation of the eight compounds (**3-10**) are depicted in Scheme 1. Dihydrothieno[3,2-c]quinoline methyl ester **7** was obtained from the aldehyde **11**,[16] after an efficient tandem S_NAr/cyclization reaction followed by elimination of water and subsequent aromatization of the thiophene ring. From compound **7**, after simple alkylation with methyl iodide, derivative **8** was afforded. Esters **7** and **8** were, in turn, hydrolyzed with sodium hydroxide and subjected to coupling reaction, in the presence of N-(3-Dimethylaminopropyl)-N′-ethylcarbodiimide hydrochloride, with the amine **12** to give compounds **3** and **4**, respectively.

Amine **12** was obtained by reacting the benzyl piperidine **14** with the N-(2-bromoethyl)phthalimide **15** affording the S_N adduct **16** that was subsequently deprotected by hydrazine yelding the 2-(4-benzylpiperidin-1-yl)ethanamine **12** (scheme 1).

In a similar way, compounds **5** and its methyl congener **6** were obtained starting from the corresponding esters **9** and **10**. The precursor aldehyde **13** came from a three steps sequence starting from the isoquinoline **17**,[17] that after a bromination reaction with N-bromosuccinimide (NBS) furnished compound **18** (Scheme 1).[18] The latter with a $NaBH_4$ reduction[19] and oxidation reaction mediated by Dess-Martin periodinane (DMP) gave the desired aldehyde **13**.

Derivative **9** was synthesized, always by a S_NAr/cyclization reaction in the presence of methylthioglycolate, starting from bromo aldehyde **13** (Scheme 1). Ester **10** is the product of the

methylation reaction of the free lactam **9**. The final amides **5** and **6** are the coupling products of amine **12** and the two carboxylic acids afforded by saponification reaction of esters **9** and **10**.

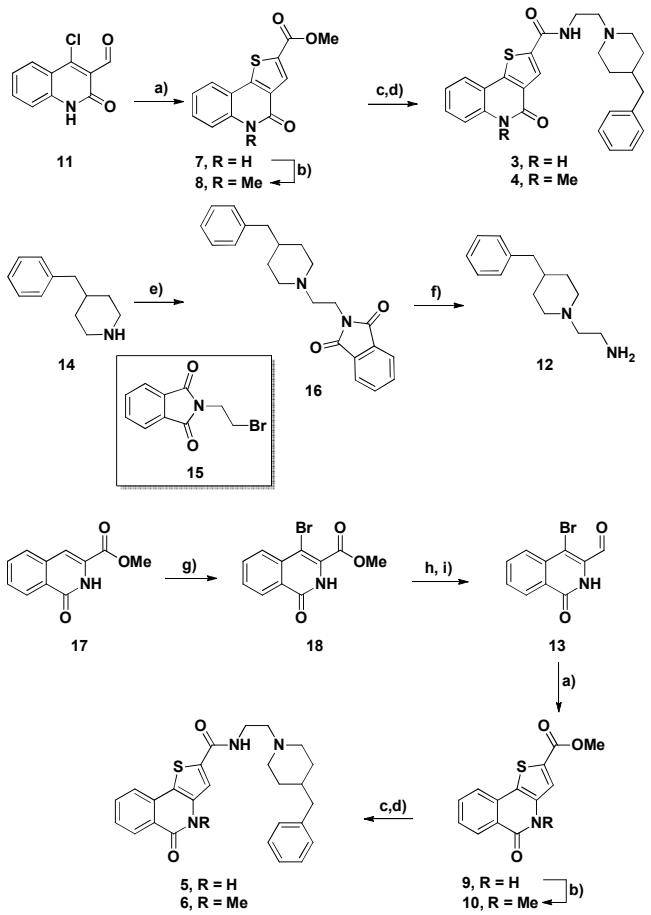

Scheme 1. Reagents a) Methyl thioglycolate, MeOH, MeONa, r.t., 18h b) MeI, DMF, K_2CO_3, 90°C, 16h c) NaOH, THF/MeOH/H_2O, r.t., 18h d) EDC, HOBt, DMF, **12**, r.t. 18h e) **15**, CH_3CN, 18h, reflux f) NH_2NH_2, MeOH, 2h, reflux g) NBS, DMF, CH_3CN, r.t., 2h h) $NaBH_4$, t-BuOH/MeOH, reflux, 2h i) DMP, $NaHCO_3$, DCM, r.t., 1h.

G4 binding and stabilization. Depending on the sequence and experimental conditions, the G-rich human telomeric DNA can fold into diverse G4 topologies.[20] Therefore, to evaluate the G4 binding properties of compounds **3-10** we considered different sequences and conditions so as to have a variety of different conformations, thereby covering most of the structural features of the possible folding topologies of telomeric DNA. In particular, for the circular dichroism

(CD) experiments we selected two different truncations of the natural human telomeric sequence, namely, the 23-nt d[TAGGG(TTAGGG)$_3$] (Tel23) and the 26-nt d[(TTAGGG)$_4$TT] (Tel26) known to form, in K^+-containing solution, referred to as hybrid-1 and hybrid-2 structures, respectively. Furthermore, several studies suggest that the predominant G4 fold is the parallel one when considering the overcrowded conditions present into a cell;[21,22] in these veins, we also prepared a Tel23 sample at high concentration of DNA to promote this G4 conformation (hereafter referred to as Tel23-p).[23] The folding adopted by each G4-forming sequence were probed by CD measurements (Supporting Information, Figures S1-S3).[24] In agreement with the presence of hybrid structures as predominant conformations, Tel23 and Tel26 showed a positive band at 289 with a shoulder at ca. 268 nm, and a weak negative band at around 240 nm in the CD spectra. Otherwise, Tel23-p showed a positive band at 264 nm and a negative one around 240 nm. Bands in the latter are characteristic of parallel-stranded G4 topologies. No substantial alterations of CD spectra were recorded for the analyzed structures upon the addition of each ligand, thus allowing to infer a general conservation of their G4 topologies. The stabilizing properties of **3**-**6** and **7**-**10** were probed by CD-melting experiments (Supporting Information, Figures S1-S3) measuring the ligand-induced change in the melting temperature (ΔT_m) of G4s. The results of these experiments (Table 1) indicate that none of the derivatives devoid of the basic chain (compounds **7**-**10**) significantly increase the stability of any G4 ($\Delta T_m \leq 3.0$ °C).

Table 1. Change in G4 DNA melting temperatures (ΔT_m) in the presence of compounds (10 mol equiv) determined by CD melting experiments.

	ΔT_m (± 1) (°C)		
Compound	**Tel23**	**Tel26**	**Tel23-p**
3	0.3	2.6	7.7
4	5.8	5.5	7.0
5	0.7	2.0	4.2
6	1.6	3.0	10.5
7	1.5	2.2	1.9
8	0.4	0.4	2.4
9	0.9	0.9	3.0
10	-0.8	1.4	1.4
19	0.0	1.1	2.4
20	0.1	1.3	2.6

Conversely, compound **4** – the one that shares the major structural similarities with the starting compound **1** – showed to appreciably enhance the stability of all the investigated telomeric G4s ($\Delta T_m \geq 5.5$ °C). On the other hand, derivatives **3** and **6** were found to stabilize to a large extent only the Tel23-p G4, with **6** that gave the highest effects showing a $\Delta T_m > 10$ °C. Indeed, for this set of compounds, the G4 ligand recognition should be mediated by the presence of a polycyclic aromatic ring that stacks on the G-quartet while cationic chains should stabilize such an interaction by engaging strong coulombic contacts with the phosphate groups of the DNA backbone. This would explain why **3**-**6** are generally more efficient in stabilizing the G4 structure if compared with the unfunctionalized compounds **7**-**10**. Once identified the compounds

that are able to increase the thermal stability of one or more telomeric G4 targets, we extended the CD melting experiments for these compounds by using a range of ligand concentrations. The thermal shift curves of the ligands followed a dose–response pattern (Figure 1). As far as Tel23-p is concerned, compounds **3** and **6** showed a similar stabilization profile (Figure 1A), whereas **4** reached its maximum stabilizing effect at a lower concentration. Dose–stabilization curves also revealed that compound **4** is significantly more effective in stabilizing Tel23-p and Tel23 G4s rather than Tel26.

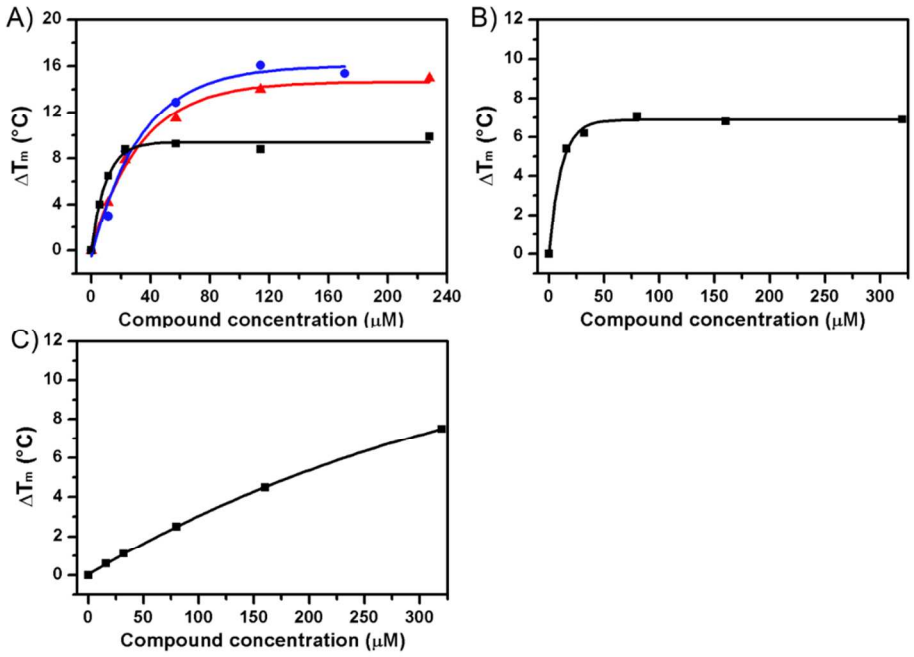

Figure 1. CD stabilization curves for (A) Tel23-p, (B) Tel23, and (C) Tel26 G4s with compounds **3** (▲), **4** (■), and **6** (●).

To evaluate any duplex stabilizing ability of **3**, **4** and **6**, CD-melting measurements were also carried out by using the self-complementary duplex-forming sequence d(CGCGAATTCGCG), showing that the selected compounds do not enhance the stability of the investigated model duplex DNA (Figure S4). Because of the structural similarities shared by these G4-targeting compounds and the PARP inhibitors, two of these, NU1025[25] (8-Hydroxy-2-methylquinazolin-

4[3*H*]-one, **19**) and olaparib[26] (4-[4-Fluoro-3-[(4-methoxypiperidin-1-yl)carbonyl]benzyl]phthalazin-1(2H)-one, 4-[[4-fluoro-3-[(4-methoxy-1-piperidinyl)carbonyl]phenyl]methyl]-1(2H)-phthalazinone, **20**), were also included in the CD melting experiments of G4s (Supporting Information, Figure S5). The data show that neither **19** nor **20** significantly increase the thermal stability of any telomeric G4 ($\Delta T_m \leq 2.6$ °C, Table 1). To obtain quantitative data related to G4–ligand binding affinity, microscale thermophoresis (MST) measurements were carried out by titrating Cy5-labeled Tel26 G4 with an increasing concentration of compound **4** (Supporting Information, Figure S6**)**. The results of these experiments indicated that **4** binds to the G4 with an equilibrium dissociation constant (K_d) of 240 (±70) nM. As a negative control, compound **8** has been titrated to the labeled G4. As expected no significant change of the thermophoretic signal is observed (Supporting Information, Figure S7).

Finally, Förster resonance energy transfer (FRET) melting analysis has been used to estimate the G4 over duplex selectivity of **4**.[27] FRET melting experiments were performed on a labeled G4-forming sequence that mimics the human telomeric overhang (F21T, see Experimental Section), in the absence or presence of a self-complementary duplex DNA sequence as competitor. FRET-melting curves of F21T (Supporting Information, Figure S8) confirmed that **4** is able to stabilize the G4 structure (ΔT_m = 4.5 °C). Moreover, compound **4** showed some selectivity for the telomeric G4 over the duplex with ΔT_m value decreases of 1.2 °C in the presence of 25-fold excess of competitor duplex (5 μM), and of 1.7 °C at the level of a 50-fold excess of the duplex (10 μM).

Targeting G4 DNA in cancer cells. The ability of compounds to target and stabilize intranuclear G4s structures in cells was assayed by staining treated cells with a monoclonal

antibody (Mab) anti-G4 (BG4). It was shown that this Mab was able to recognize more G4s when cells are exposed to G4 stabilizers.[28] In cells treated with compounds **1, 3, 4**, and **6-10**, we observed an increased anti-G4 staining (Figure 2) that nicely correlated with the ability of compounds to bind to G4 DNA *in vitro*. On the other hand, no anti-G4 staining was observed in cells treated with a PARP and Tankyrase inhibitor, **20** and XAV939[29] (3,5,7,8-Tetrahydro-2-[4-(trifluoromethyl)phenyl]-4H-thiopyrano[4,3-d]pyrimidin-4-one, **21**), respectively.

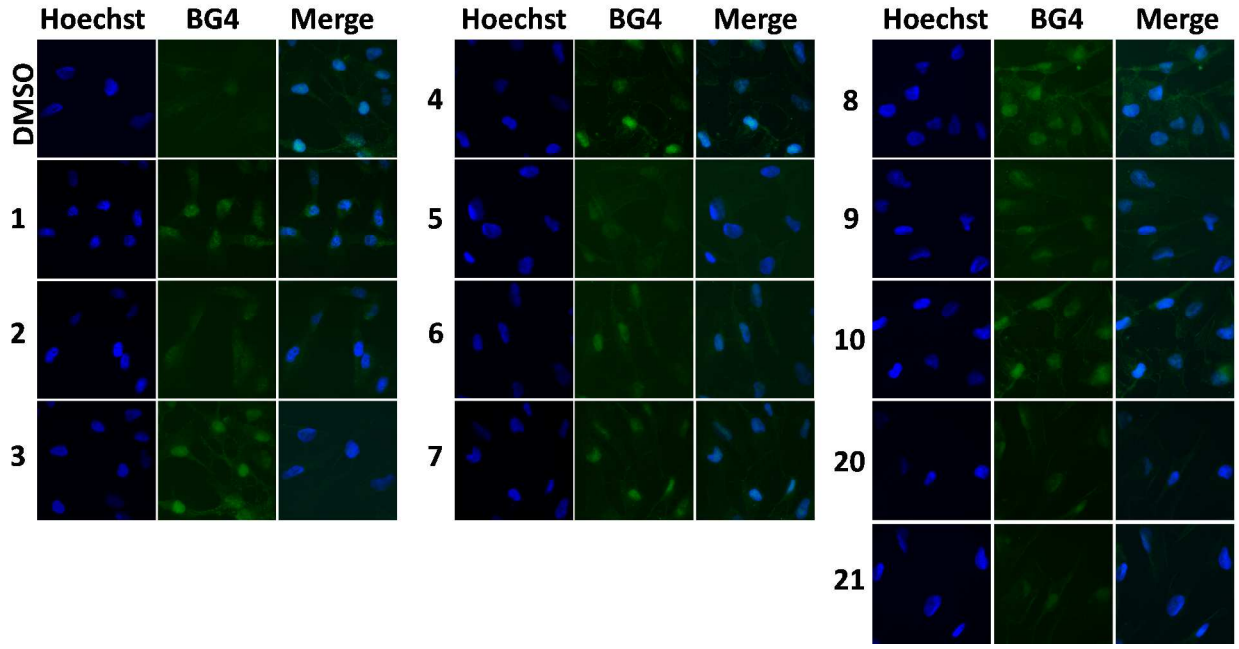

Figure 2. *In cellulo* G4s stabilization. BJ-EHLT cells were treated with 1 μM of each compound for 24 hours. At the end of treatment, cells were fixed and immunostained with the Mab anti-G4 (BG4) and with a FITC conjugated Goat anti-Mouse secondary antibody. Finally, cells were counterstained with Hoechst to mark nuclei. Images were acquired at 63X magnification.

Besides its role as *in vitro* telomerase inhibitor, G4 stabilization was shown to trigger a rapid DDR activation at telomere level, which is responsible for the short-term anti-proliferative effect.[30] To further ascertain the *in cellulo* ability of the newly generated compounds to target G4 structures, the activation of DDR in nuclei of normal telomerized fibroblasts (BJ-hTERT) or

transformed human fibroblasts (BJ-EHLT) was measured by immunofluorescence staining against γH2AX (a hallmark of DNA double strand breaks). After 24 hours exposure to 1 μM concentrations, compounds **3**, **4**, **6**, **7** and **10** revealed a significant increase in the percentage of nuclei displaying γH2AX foci (Figure 3A) and a preferential effect on transformed vs normal fibroblasts, similarly to the already reported G4 ligand **1**.[14] As expected, the PARP inhibitor parent compound **2,** did not show any G4 stabilization (Figure 2) neither DDR activation properties (Figure 3) in cells. Higher doses of compounds **8** and **9** were tested without observing any further increase of DDR activation (data not shown). The telomere targeting effect of compounds **3**, **4**, **6**, **7** and **10**, in comparison with **1** was then assayed in terms of ability to induce Telomere's Dysfunction Induced Foci (TIFs), revealed as co-localizing foci in nuclei co-immunolabeled with γH2AX and the telomere marker TRF1. The percentage of TIFs positive nuclei was significantly increased by **1**, **3**, **4** and **6**, but not by **7** and **10**. Of note, compound **4** resulted in being the most effective telomere targeting molecule (Figures 3B and 3C). Indeed, a certain correlation was recorded between the ability of the tested compounds to reach the G4 in cells and their potential to induce a DDR at telomere level.

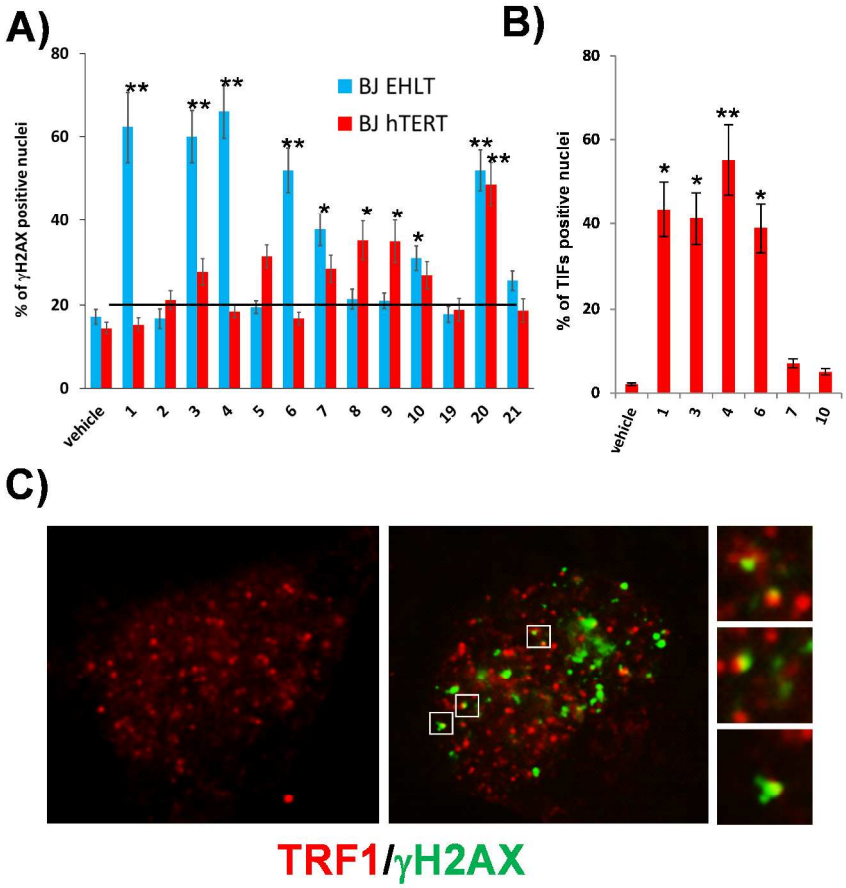

Figure 3. DDR and telomere's dysfunction induction. Histograms in A report the percentage of BJ-EHLT and BJ-hTERT fibroblasts γH2AX positive nuclei or the percentage of nuclei containing more than 4 γH2AX/TRF1 co-localizations (considered as TIFs positive, B) in the most effective conditions. Pictures in C show representative images of co-localizations at 100X magnification and 8X enlargements. Histograms show the mean values of three independent experiments while images show one representative of three independent experiments with similar results. Bars indicate means ± SD. *=p<0.1; **= p<0.01.

Effect on poly(ADP-ribosyl)ation (PARylation). To understand if any of the modifications introduced by the synthesis could also confer PARPi properties to the newly generated compounds, we tested for their ability to affect the PARylation reaction in cultured cells. To this

aim, compounds were administered for 16 hours to fibroblast cultures and then incorporation of radiolabeled $NADH^+$ into ADP-ribose polymers (PARs) was measured as a result of the PARP catalytic activity. The highest inhibition of PARP activity was achieved by compound **5** that shows an *in cellulo* effect comparable to the clinically employed PARP inhibitor (PARPi) **20** (Figure 4) with an *in vitro* IC_{50} inhibition of 223 nM against purified PARP1 (Supporting Information, Figure S9).

In this respect, it should be pointed out that for analogous compounds (**2**) extensive structure-activity studies (SARs), supported by molecular modeling inspections,[15] have already outlined that in the interaction with PARPs the ligand lactam group engages a bidentate H-bond interaction with the enzyme counterpart. This should explain why reverting the lactam (**3**) and/or methylating the endocyclic nitrogen (**4** and **6**) results in a comparably lower PARPs inhibiting potency.

Given the role of PARP1 in DNA damage repair, we analyzed the timing of DDR resolution after compounds removal. Figure S10 of Supporting Information shows that DNA damage is rapidly recovered after removal of all the compounds, included those with PARPi activity. This indicates that both DDR activation and PARP inhibition are completely reversible after removing the compounds.

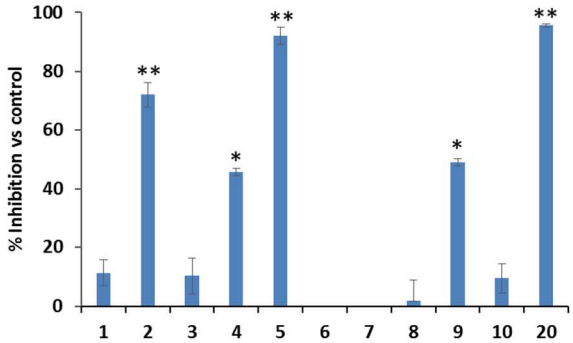

Figure 4. PARP activity assays. BJ-EHLT cells were exposed to 1 μM of each compound for 16 hours. Then, cells were permeabilized with digitonin and incubated with ^{3}H-NAD. Radiolabelled PARs were precipitated with trichloroacetic acid (TCA) and quantified by a scintillation counter. Histograms report the inhibition of PARylation exerted by the different compounds *vs* DMSO-treated samples. Histograms show the mean values of three independent experiments. Bars indicate means ±SD. *=$p<0.1$; **= $p<0.01$.

Cytotoxicity of 4 and 5 in BRCA2 deficient cell line. The advantage of having generated a single molecule able to induce a G4 stabilization and contemporarily to impair the DNA repair process could enable us to substitute combinatory treatments[12] with a single agent. Tumors with germline or acquired mutations in BRCA1 and BRCA2 genes were shown to be preferentially susceptible to PARPi inhibition, and more recently, to some G4-ligands.[31] While the single G4 binder **1** has the same effect in both BRCA2 proficient and deficient DLD1 colon cancer cells, whereas, at the same doses, compound **2** has no antiproliferative effect in both cell lines.[32] This is in agreement with the lower PARPi activity of compound **2** in the *in-vivo* assay, and with a reported modest anti-proliferative effect in absence of stimuli. On the other hand, the acquisition of even a partial PARPi capacity is able to confer to compound **4** the same ability of a pure PARPi (compound **5**) to preferentially kill BRCA2 deficient cells. This encourages further optimization of the dual compound **4** for pre-clinical studies.

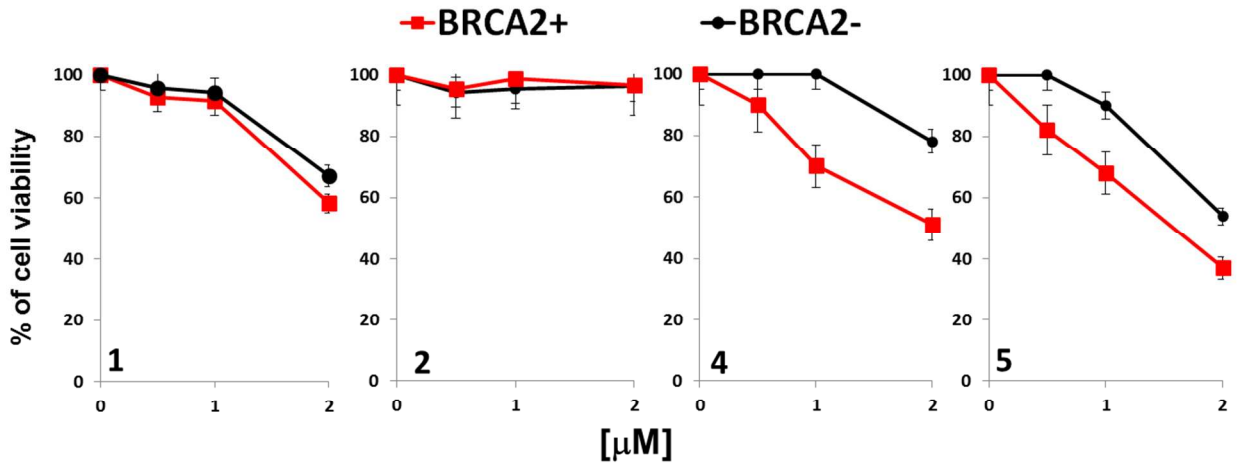

Figure 5. BRCA2 proficient and deficient DLD1 colon cancer cell lines were exposed to the indicated concentrations of compounds **1**, **2**, **4**, and **5** and cell viability was determined by MTT assay after 6 days of drug exposure.

Conclusions.

Considering the synergistic effect of G4 stabilization and PARP1 inhibition on tumor cells and the intrinsic advantages of multiple-target drugs over combination therapies, herein we aimed at identifying the first chemotypes that are able to have this dual mechanism of action. Of the newly designed compounds, **4** demonstrated efficient G4 stabilizing properties, sufficient anti-PARP activity in cells as well as interesting antiproliferative potential in cancer cells. Future medicinal chemistry efforts will be aimed at optimizing the inhibitory activity of our lead **4** against PARP isoenzymes while maintaining the affinity and stabilizing properties for G4 DNA. These studies will take advantage of recent studies by some of us outlining how the synthesis of compound **4** derivatives is amenable to the application of a multi-step continuous flow synthesis approach.[33]

Experimental Section.

1. Chemistry.

General Methods. All the compounds were characterized by ^{1}H and ^{13}C NMR and MS analysis. NMR spectra were recorded at a 400 MHz spectrometer. Chemical shifts (δ) are reported relative to $CDCl_3$ at δ 7.26 ppm, CD_3OD δ 3.30 or $(CD_3)_2SO$ at δ 2.50 ppm and tetramethylsilane at δ 0.00 ppm. Chemical shifts are reported in part per million (ppm) relative to the residual solvent peak (see Supporting Information). Mass spectral (MS) data were obtained using a LC/MS system with a 0.4 mL/min flow rate using a binary solvent system of 95:5 methyl alcohol/ water. UV detection was monitored at 254 nm. Mass spectra were acquired in positive mode scanning over the mass range of 50-1500. The following ion source parameters were used: drying gas flow, 9 mL/min; nebulizer pressure, 40 psig; drying gas temperature, 350 °C. On the basis of HPLC analysis, all final compounds have a purity ranging from 96 to 98%.

General procedure for the synthesis of the esters 7 and 9.[34] A mixture of methyl thioglycolate (5.05 mmol), 20% solution of NaOMe in MeOH (5.05 mmol), and MeOH (5 mL) was stirred at room temperature for 10 min. The opportune aldehyde (2.53 mmol) was added and the mixture was stirred at room temperature for 18 h. The mixture was acidified with 1 M HCl and the resulting mixture was stirred for 30 min. The precipitated solid was collected by filtration, washed with water and Et_2O to give the title compound.

General procedure for the synthesis of the methyl derivatives 8 and **10.** Methyl Iodide (1.67 mmol) was added dropwise to a suspension of **16** (1.5 mmol) in DMF (15 mL) and K_2CO_3 (2.2 mmol). The mixture was heated at 90 °C and stirred for 16 h. After this time the suspension was diluted with H_2O and extracted three times with AcOEt. The combined organic extracts were washed with brine, dried over Na_2SO_4, and concentrated in vacuo. The residue was purified by silica gel chromatography (hexane/AcOEt = 1/1).

General procedure for the synthesis of the amides 3-6. A solution of the opportune ester (1.35 mmol) and 2 M NaOH (6 mL) in THF (20 mL)/MeOH (10 mL) was stirred at room temperature for 18 h. The reaction mixture was neutralized with 1 M HCl, and the resulting solid was collected by filtration. The solid was washed with water and Et_2O to give the title compound that was used for the next step without further purifications. EDC (0.49 mmol) was added to a mixture of the opportune carboxylic acid (0.33 mmol), amine **12** (0.49 mmol), and HOBt (0.49 mmol) in DMF (4 mL), and the mixture was stirred at room temperature for 18 h. The reaction mixture was diluted with saturated $NaHCO_3$ aq. The precipitated solid was collected by filtration, washed with water and Et_2O to give the title compound.

Methyl 4-bromo-1-oxo-1,2-dihydroisoquinoline-3-carboxylate (18). To a solution of ester **17** (8.17 mmol) in a mixture of DMF (20 ml) and acetonitrile (3 mL) was added NBS (8.58 mmol). After 2 h the reaction mixture was diluted with s.s.NaHCO3 (30 mL) and extracted with EtOAc (3 x 30 mL). The combined organic extracts were washed with brine, dried over $MgSO_4$, and concentrated in vacuo. The residue was purified by basic silica gel column chromatography (Hexane/ EtOAc= 3/1 to 1/1).

4-bromo-1-oxo-1,2-dihydroisoquinoline-3-carbaldehyde (13). The ester (17, 2.38 mmol) and sodium borohydride (3.6 mmol) were heated in refluxing mixture of tert-butanol (3mL) and methanol (0.6 mL) for 2 hours. After this time, the cooled mixture was partitioned between EtOAc and H_2O. The aqueous phase was re-extracted with EtOAc and the combined organics were washed with brine, dried and evaporated to give the title compound. The alcohol so obtained was dissolved in DCM (0,1M), $NaHCO_3$ (1.5 eq.) and DMP (1.2 eq.) were added and the mixture was stirred at room temperature for 1 h. The reaction mixture was diluted with H_2O (10ml) and extracted with DCM (3 x 10 mL). The combined organic extracts were washed with

brine, dried over $MgSO_4$, and concentrated in vacuo. The residue was purified by basic silica gel column chromatography (Hexane/ EtOAc= 3/1).

2-(4-benzylpiperidin-1-yl)ethanamine (16).[35] A mixture of benzyl piperidine **14** (10 mmol) and N-(2-bromoethyl)phthalimide **15** (10 mmol) in 50 mL of acetonitrile was stirred under reflux for 18 h. The crystalline precipitate formed was collected and recrystallized from EtOH to give **16** as a colorless solid.

2-(4-benzylpiperidin-1-yl)ethanamine (12). A mixture of **16** (7 mmol) and hydrazine hydrate (10 mmol) in MeOH (50 mL) was stirred under reflux for 2 h. After cooling the reaction mixture was filtered and evaporated. Dissolution of the residue in 1 M NaOH (30 mL), extraction with EtOAc (3 x 30 mL), drying and evaporation gave **12**. The product was enough pure to be used without further purification.

2. Oligonucleotide synthesis, sample preparation, and CD experiments. The DNA sequences were synthesized using standard β-cyanoethylphosphoramidite solid phase chemistry[36] on an ABI 394 DNA/RNA synthesizer (Applied Biosystem) at the 5-μmol scale. DNA detachment from support and deprotection were performed by treatment with concentrated ammonia aqueous solution at 55 °C for 12 h. The combined filtrates and washings were concentrated under reduced pressure, dissolved in water, and purified by high-performance liquid chromatography (HPLC) on a Nucleogel SAX column (Macherey-Nagel, 1000-8/46), using buffer A consisting of 20 mM KH_2PO_4/K_2HPO_4 aqueous solution (pH 7.0), containing 20% (v/v) CH_3CN, buffer B consisting of 1 M KCl, 20 mM KH_2PO_4/K_2HPO_4 aqueous solution (pH 7.0), containing 20% (v/v) CH_3CN, and a linear gradient from 0% to 100% B for 30 min with a flow rate 1 mL/min. The fractions of the oligomers were collected and successively desalted by Sep-pak cartridges (C-18). The isolated oligonucleotides were proved to be > 98%

pure by NMR. In particular, the following oligonucleotides have been synthesized and used for the CD experiments: d[TAGGG(TTAGGG)$_3$] (Tel23), d[(TTAGGG)$_4$TT] (Tel26), and d(CGCGAATTCGCG). The concentration of oligonucleotides was determined by UV adsorption measurements at 90 °C using appropriate molar extinction coefficient values ε (λ = 260 nm) calculated by the nearest neighbor model.[37] Tel23 and Tel26 G4s were prepared in 10 mM lithium phosphate buffer (pH 7.0) containing 70 mM KCl. Samples were heated at 90 °C for 5 min, and then gradually cooled to room temperature overnight. Tel23 G4 in the parallel arrangement (Tel23-p) was prepared in 10 mM lithium phosphate (pH 7.0), 100 mM KCl, as previously described.[38] Finally, d(CGCGAATTCGCG)$_2$ duplex (ds12) was prepared in 20 mM sodium phosphate buffer (pH 7.0), 200 mM NaCl, and annealed as reported above. CD experiments were performed on a Jasco J-815 spectropolarimeter equipped with a PTC-423S/15 Peltier temperature controller. CD spectra were recorded at 20 and 90 °C (before and after melting experiment, respectively) in the 230-360 nm wavelength range. The scan rate was set to 100 nm/min, with a 1 s response time, and 1 nm bandwidth. The CD spectra were averaged over three scans, smoothed and zero corrected. Buffer baseline was subtracted from each spectrum. 10-16 μM G4s and 21 μM duplex DNA were used. Aliquots of ligands (10 mM in DMSO) were added to achieve the desired equivalent proportions. CD spectra were recorded 30 min after ligand addition. CD melting was carried out in the 20-100 °C temperature range, at 1 °C/min heating rate by following changes of CD signal at the wavelength of the maximum CD intensity. CD melting experiments were recorded in the absence and presence of ligands added to the pre-folded DNA structures.[39] The melting temperatures were determined from curve fit using Origin 7.0 software (http://www.originlab.com). ΔT_m values were determined as the difference in melting temperature between the DNA with and without ligands.

3. Microscale thermophoresis experiments. Microscale thermophoresis (MST) measurements were performed using the Monolith NT.115 (Nanotemper Technologies, Munich, Germany). The labeled Tel26 oligonucleotide (Cy5, Biomers) was prepared in 10 mM lithium phosphate buffer (pH 7.0) containing 70 mM KCl supplemented with 0.05% Tween and 2-4% DMSO as final concentration. The concentration of the labeled oligonucleotide was kept constant at 30 nM, while a serial dilution of the investigated compound in the same buffer was prepared and mixed with the oligonucleotide solution with a volume ratio of 1:1. Samples were loaded into standard capillaries (NanoTemper Technologies). Measurements were performed at 20 °C, using 40 or 60% LED and 40 or 60% MST power. MST data analysis was performed by employing the PALMIST software using the 1:1 fitting model.[40] The plots were rendered with GUSSI v1.2.1 software (http://biophysics.swmed.edu/MBR/software.html).

4. FRET melting experiments. The FRET melting assay was carried out on a FP-8300 spectrofluorometer (Jasco) equipped with a Peltier temperature controller accessory (Jasco PCT-818). The experiments were performed by using the G4 forming sequence 5'-FAM-d(GGG[TTAGGG]3)-TAMRA-3' (F21T),[41] which had covalently attached the donor fluorophore FAM (6-carboxyfluorescein) and the acceptor fluorophore TAMRA (6-carboxytetramethylrhodamine). Labeled oligonucleotide was purchased from Biomers (Germany) and purified employing standard HPLC protocols. F21T was prepared as a 1 μM solution in K^+ buffer and then annealed by heating to 90 °C for 5 min, followed by cooling to room temperature overnight. Measurements were made with excitation at 492 nm and detection at 522 nm. Both excitation and emission slit widths were set at 5 nm. A sealed quartz cuvette with a path length of 1 cm was used. The final concentration of F21T G4 was 0.2 μM. Experiments were performed in the presence of compound 4 (4.0 μM) without and with 5.0 and

10.0 μM double-stranded DNA (ds12) competitor. In addition, a blank with no compound or competitor was also analyzed. The fluorescence melting of G4 was monitored at 1 °C/min over the range 20-90 °C. Emission of FAM was normalized between 0 and 1. Final analysis of the data was carried out using Origin 7.0 software.

5. Cells and Culture Conditions. BJ fibroblasts expressing hTERT and SV40 early region (BJ-HELT), were obtained as previously reported.[42] BRCA2 deficient and proficient DLD1 colon cancer cell lines were obtained by Madalena Tarsounas. Cells were grown in Dulbecco Modified Eagle Medium (D-MEM, Invitrogen Carlsbad, CA, USA) supplemented with 10% fetal calf serum, 2 mM L-glutamine and antibiotics. For cell treatments, compounds were dissolved in DMSO at 1 mg/ml concentration and, then, diluted into cell culture medium. Compound **1** was acquired by purchased by ChemDiv while compound **2** was acquire by Sigma Aldrich. DMSO treated cells were used as a control.

6. Immunofluorescence. Cells were fixed in 2% formaldehyde and permeabilized in 0.25% Triton X 100 in PBS for 5 min at room temperature. For immunolabeling, cells were incubated with the primary antibodies, then washed in PBS and incubated with the secondary antibodies and counterstained by Hoechst (Sigma) to mark nuclei. The following primary antibodies were used: pAb anti-TRF1 (Abcam Ltd.; Cambridge UK); mAb anti-γH2AX (Upstate, Lake Placid, NY); Mab anti-DNA/RNA G-quadruplex BG4 (Absolute antibody). The following secondary antibody were used: TRITC conjugated Goat anti-Rabbit, FITC conjugated Goat anti-Mouse (Jackson ImmunoResearch Europe Ltd., Suffolk, UK). Fluorescence signals were recorded by using a Leica DMIRE2 microscope equipped with a Leica DFC 350FX camera and elaborated by a Leica FW4000 deconvolution software (Leica, Solms, Germany). This system permits to focus single planes inside the cell generating 3D high-resolution images. For quantitative analysis of

γH2AX positivity, 200 cells on triplicate slices were scored. For TIF analysis, in each nucleus, a single plane was analyzed and at least 50 nuclei per sample were scored.

7. Cell-based PARP activity assays. For the analysis of in-vivo PARP activity, cells ($5x10^5$ cells) were exposed to 1 μM of the compounds under study or DMSO for 12 hrs. Medium was then replaced by 0.5 ml PARP buffer (56 mM Hepes pH 7.5, 28 mM KCl, 28 mM NaCl, 2 mM $MgCl_2$, 0.01% digitonin, and 0.125 μM NAD and 0.5 μCi/ml ^{3}H-NAD (Perkin-Elmer, Milan, Italy) and plates were incubated for 10 min at 37 °C. Cells were then scraped, recovered in microtubes and then precipitated using TCA for 3 hrs at 4°C. Samples were then spun and the pellets washed twice in ice-cold 5% TCA and solubilized overnight in 2% SDS/0.1 N NaOH at 37 °C. Contents of the tubes were added to 7 ml ScintiSafe Plus scintillation liquid (Fisher Scientific) and radioactivity was determined in a liquid scintillation counter (Wallac; Gaithersburg, MD). Data were expressed as mean ± SD of triplicate samples.

8. Cell-free PARP-1 activity assay. The assay was performed in order to calculate the IC_{50} of compound **5** and the PARPi **20** on the activity of the purified PARP-1 protein. Three units of purified PARP-1 (High Specific Activity, Trevigen, Gaithersburg, MD), untreated or exposed to graded concentrations (1 nM – 1 μM) of compound **5** or **20**, were incubated in the presence of 1 μCi ^{32}P-NAD^+ (PerkinElmer), 200 μM NAD^+, 1x PARP-1 buffer (100 mM Tris-HCl, 10 mM $MgCl_2$, 2 mM DTT), 10 μg of nuclease-treated salmon testes DNA (Trevigen), 10 μg of histones (Merck Millipore). The reaction mixture was incubated on ice for 15 minutes at room temperature. At the end of the incubation, ribosylated proteins were precipitated by the addition of 20% TCA and the radioactivity was quantified by a scintillation counter.

9. Cell viability assay. To determine cell viability, MTT assay was performed in treated and untreated cells (parental and BRCA2-mutated, Horizon Discovery at. AQ5 MN, USA) for 24 h.

Cells were incubated with MTT solution (Sigma-Aldrich), and the purple formazan crystals were dissolved in isopropanol. OD at 540 nm AQ5 was determined on a microplate reader.

ASSOCIATED CONTENT

Supporting Information. Characterization of all the compounds; CD spectra; CD- and FRET-melting curves; MST plots; PARP1 *in vitro* inhibition dose-response plot; DDR recovery experiment plot. This material is available free of charge via the Internet at http://pubs.acs.org.

AUTHOR INFORMATION

Corresponding Authors

*S.C. Phone: +39 0823 274789. E-mail: sandro.cosconati@unina2.it. *E.C. Phone: +39 06 5266 5520. E-mail: erica.salvati@gmail.com.

Author Contributions

The manuscript was written through contributions of all authors. All authors have given approval to the final version of the manuscript. [£]These authors contributed equally to this work.

Funding Sources

This work was supported by Regione Campania under POR Campania FESR 2007-2013 - O.O. 2.1 (FarmaBioNet) and Progetti di Rilevante Interesse Nazionale (PRIN) 2012 (grant no. 2012CTAYSY_002) by the Italian MIUR (PRIN 2012) to S.C.; by the Italian Association for Cancer Research (AIRC) (IG-14150 to A.R., IG-16730 to B.P., MFAG-17121 to E.S. and IG-16910 to A.B); and by “Programma STAR” 2014 of University of Naples "Federico II" to B.P. (#14-CSP3-C03-141).

ABBREVIATIONS

ALT, alternative lengthening of telomere; G4, G-quadruplex; TOP1, Topoisomerase I; TOPIIIα Topoisomerase IIIα; PARPs, poly(ADP-ribose) polymerases; TNKS, Tankyrase; CD, circular dichroism; Förster resonance energy transfer, FRET; DDR, DNA damage response; TIFs, Telomere's Dysfunction Induced Foci; PARPi, poly(ADP-ribose) polymerase inhibitor.

REFERENCES

1. de Lange, T. Shelterin: the protein complex that shapes and safeguards human telomeres. *Genes Dev.* **2005**; *19*, 2100–2110.
2. Blackburn, E. H. Switching and signaling at the telomere. *Cell* **2001**, *106*, 661–673.
3. Lin, S. Y.; Elledge, S. J. Multiple tumor suppressor pathways negatively regulate telomerase. *Cell* **2003**, *113*, 881–889.
4. Kim, N.; Piatyszek, M.; Prowse, K.; Harley, C.; West, M.; Ho, P.; Coviello, G.; Wright, W.; Weinrich, S.; Shay, J. W. Specific association of human telomerase activity with immortal cells and Cancer. *Science* **1994**, *266*, 2011–2015
5. Cesare, A. J.; Reddel, R. R. Telomere uncapping and alternative lengthening of telomeres. *Mech. Ageing Dev.* **2008**, *129*, 99–108.
6. Bodnar, A. G.; Ouellette, M.; Frolkis, M.; Holt, S. E.; Chiu, C. P.; Morin, G. B.; Harley, C. B.; Shay, J. W.; Lichtsteiner, S.; Wright, W. E. Extension of life-span by introduction of telomerase into normal human cells. *Science* **1998**, *279*, 349–352.
7. Palm, W.; de Lange, T. How shelterin protects mammalian telomeres. *Annu. Rev. Genet.* **2008**, *42*, 301–334.

8. Bochman, M. L.; Paeschke, K.; Zakian, V. A. DNA secondary structures: stability and function of G-quadruplex structures. *Nat. Rev. Genet.* **2012**, *13*, 770–780.
9. Gomez, D.; O'Donohue, M. F.; Wenner, T.; Douarre C.; Macadré J.; Koebel, P.; Giraud-Panis, M. J.; Kaplan, H.; Kolkes, A.; Shin-ya, K.; Riou, J. F. The G-quadruplex ligand telomestatin inhibits POT1 binding to telomeric sequences in vitro and induces a GFP-POT1 dissociation from telomeres in human cells. *Cancer Res*. **2006**, *66*, 6908–6912.
10. De Cian, A.; Lacroix, L.; Douarre, C.; Temime-Smaali, N.; Trentesaux, C.; Riou, J.-F.; Mergny, J.-L. Targeting telomeres and telomerase. *Biochimie* **2008**, *90*, 131–155.
11. Neidle, S. Quadruplex nucleic acids as novel therapeutic targets. *J. Med. Chem*. **2016**, *59*, 5987–6011.
12. Salvati, E.; Scarsella, M.; Porru, M.; Rizzo, A.; Iachettini, S.; Tentori, L.; Graziani, G.; D'incalci, M.; Stevens, M. F. G.; Orlandi, A.; Passeri, D.; Gilson, E.; Zupi, G.; Leonetti, C.; Biroccio, A. PARP1 is activated at telomeres upon G4 stabilization: possible target for telomere-based therapy. *Oncogene* **2010**, *29*, 6280–6293.
13. a) Monzon, J. G.; Dancey, J. Combination agents versus multi-targeted agents– pros and cons. In *Designing Multi-Target Drugs*; Morphy, J. R.; Harris, C. J., Eds.; RSC Publishing: Cambridge, 2012; pp 155–181. b) Anighoro, A.; Bajorath, J.; Rastelli, G. Polypharmacology: challenges and opportunities in drug discovery. *J. Med. Chem.* **2014**, *57*, 7874–7887.
14. Di Leva, F. S.; Zizza, P.; Cingolani, C.; D'Angelo, C.; Pagano, B.; Amato, J.; Salvati, E.; Sissi, C.; Pinato, O.; Marinelli, L.; Cavalli, A.; Cosconati, S.; Novellino, E.; Randazzo, A.; Biroccio, A. Exploring the chemical space of G-quadruplex binders: discovery of a

novel chemotype targeting the human telomeric sequence. *J. Med. Chem.* **2013**, *56*, 9646–9654.

15. Pellicciari, R.; Camaioni, E.; Costantino, G.; Marinozzi, M.; Macchiarulo, A.; Moroni, F.; Natalini, B. Towards new neuroprotective agents: design and synthesis of 4H-thieno[2,3-c] isoquinolin-5-one derivatives as potent PARP-1 inhibitors. *Farmaco* **2003**, *58*, 851–858.
16. Chilin, A.; Marzaro, G.; Marzano, C.; Via, L. D.; Ferlin, M. G.; Pastorini, G.; Guiotto, A. Synthesis and antitumor activity of novel amsacrine analogs: the critical role of the acridine moiety in determining their biological activity. *Bioorg. Med. Chem.* **2009**, *17*, 523–529.
17. Nunami, K.; Suzuki, M.; Yoneda, N. One-step synthesis of 1-oxo- 1,2-dihydroisoquinoline-3-carboxylic acid derivatives. *J. Org. Chem.* **1979**, *44*, 1887–1888.
18. Kuduk, S. D.; Beshore, D.C.; Yang, Z.S. Isondolone M1 Receptor positive allosteric modulators PCT/US2001/041933 (WO/2012/003147), 2012.
19. Brooks, G.; Davies, D.T.; Jones, G.E.; Markwell, R.E.; Pearson, N. D. Nitrogen-containing bicyclic heterocycles for use as antibacterials PCT/EP2002/005708 (WO/2003/087098 A1), 2003.
20. Dai, J.; Carver, M.; Yang, D. Polymorphism of human telomeric quadruplex structures. *Biochimie* **2008**, *90*, 1172–1183.
21. a) Parkinson, G. N.; Lee, M. P.; Neidle, S. Crystal structure of parallel quadruplexes from human telomeric DNA. *Nature* **2002**, *417*, 876-880. b) Pagano, B.; Cosconati, S.; Gabelica, V.; Petraccone, L.; De Tito, S.; Marinelli, L.; La Pietra, V.; Di Leva, FS.; Lauri, I.; Trotta, R.; Novellino, E.; Giancola, C.; Randazzo A. State-of-the-art

methodologies for the discovery and characterization of DNA G-quadruplex binders. *Curr. Pharm. Des.* **2012**, *18*, 1880–1899.

22. Xue, Y.; Kan, Z. Y.; Wang, Q.; Yao, Y.; Liu, J.; Hao, Y. H.; Tan, Z. Human telomeric DNA forms parallel-stranded intramolecular G-quadruplex in K^+ solution under molecular crowding condition. *J. Am. Chem. Soc.* **2007**, *129*, 11185–11191.
23. Pagano, B.; Amato, J.; Iaccarino, N.; Cingolani, C.; Zizza, P.; Biroccio, A.; Novellino, E.; Randazzo, A. Looking for efficient G-quadruplex ligands: Evidence for selective stabilizing properties and telomere damage by drug-like molecules. *ChemMedChem* **2015**, *10*, 640–649.
24. (a) Masiero, S.; Trotta, R.; Pieraccini, S.; De Tito, S.; Perone, R.; Randazzo, A.; Spada, G.P. A non-empirical chromophoric interpretation of CD spectra of DNA G-quadruplex structures. *Org. Biomol. Chem.* **2010**, *8*, 2683-2692; (b) Karsisiotis, A.I.; Hessari, N.M.; Novellino, E.; Spada, G.P.; Randazzo, A.; Webba da Silva, M. Topological characterization of nucleic acid G-quadruplexes by UV absorption and circular dichroism. *Angew. Chem. Int. Ed. Engl.* **2011**, *50*,10645-10648; (c) Randazzo, A.; Spada, G. P.; Webba Da Silva, M. Circular dichroism of quadruplex structures. *Top. Curr. Chem.* **2013**, *330*, 67–86.
25. Bowman, K.J.; White, A.; Golding, B.T.; Griffin, R.J.; Curtin, N.J. Potentiation of anti-cancer agent cytotoxicity by the potent poly(ADP-ribose) polymerase inhibitors NU1025 and NU1064. *Br. J. Cancer*. **1998**. *78*, 1269–1277.
26. Menear, K.A.; Adcock, C.; Boulter, R.; Cockcroft, X.L.; Copsey, L.; Cranston, A.; Dillon, K.J.; Drzewiecki, J.; Garman, S.; Gomez, S.; Javaid, H.; Kerrigan, F.; Knights, C.; Lau, A.; Loh, V.M. Jr.; Matthews, I.T.; Moore, S.; O'Connor, M.J.; Smith, G.C.;

Martin, N.M. 4-[3-(4-cyclopropanecarbonylpiperazine-1-carbonyl)-4-fluorobenzyl]-2H-phthalazin-1-one: a novel bioavailable inhibitor of poly(ADP-ribose) polymerase-1. *J. Med. Chem*. **2008**, *51*, 6581–6591.

27. Giancola, C.; Pagano, B. Energetics of ligand binding to G-quadruplexes. *Top. Curr. Chem.* **2013**, *330*, 211−242.
28. Biffi, G.; Tannahill, D.; McCafferty, J.; Balasubramanian S. Quantitative visualization of DNA G-quadruplex structures in human cells. *Nat. Chem.* **2013**, *5,* 182−186.
29. Huang, S.M.; Mishina, Y.M.; Liu, S.; Cheung, A.; Stegmeier, F.; Michaud, G.A.; Charlat, O.; Wiellette, E.; Zhang, Y.; Wiessner, S.; Hild, M.; Shi, X.; Wilson, C.J.; Mickanin, C.; Myer, V.; Fazal, A.; Tomlinson, R.; Serluca, F.; Shao, W.; Cheng, H.; Shultz, M.; Rau, C.; Schirle, M.; Schlegl, J.; Ghidelli, S.; Fawell, S.; Lu, C.; Curtis, D.; Kirschner, M.W.; Lengauer, C.; Finan, P.M.; Tallarico, J.A.; Bouwmeester, T.; Porter, J.A.; Bauer, A., Cong, F. Tankyrase inhibition stabilizes axin and antagonizes Wnt signalling. *Nature*. **2009**, *461*, 614–620.
30. Salvati, E.; Leonetti, C.; Rizzo, A.; Scarsella, M.; Mottolese, M.; Galati, R.; Sperduti, I.; Stevens, M. F.; D'Incalci, M.; Blasco, M.; Chiorino, G.; Bauwens, S.; Horard, B.; Gilson, E.; Stoppacciaro, A.; Zupi, G.; Biroccio, A. Telomere damage induced by the G-Quadruplex ligand RHPS4 has an antitumor effect. *J. Clin. Invest.* **2007**, *117*, 3236–3247.
31. Zimmer, J.; Tacconi, E.M.; Folio, C.; Badie, S.; Porru, M.; Klare, K.; Tumiati, M.; Markkanen, E.; Halder, S.; Ryan, A.; Jackson, S. P.; Ramadan, K.; Kuznetsov, S. G.; Biroccio, A.; Sale, J. E.; Tarsounas, M. Targeting BRCA1 and BRCA2 deficiencies with G-quadruplex-interacting compounds. *Mol. Cell*. **2016**, *61*, 449–460.

32. Kim, H.; Tarhuni, A.; Abd Elmageed, Z.Y.; Boulares, A.H. Poly(ADP-ribose) polymerase as a novel regulator of 17β-estradiol-induced cell growth through a control of the estrogen receptor/IGF-1 receptor/PDZK1 axis. *J. Transl. Med.* **2015,** *13*, 233.

33. Filipponi, P.; Ostacolo, C.; Pellicciari, R.; Gioiello, A. Continuous flow synthesis of thieno[2,3-c]isoquinolin-5(4H)-one scaffold: a valuable source of PARP-1 inhibitors. *Org. Process Res. Dev.* **2014**, *18*, 1345–1353.

34. Ohashi, T.; Oguro, Y.; Tanaka, T.; Shiokawa, Z.; Shibata, S.; Sato, Y.; Yamakawa, H.; Hattori, H.; Yamamoto, Y.; Kondo, S.; Miyamoto, M.; Tojo, H.; Baba, A.; Sasaki, S. Discovery of pyrrolo[3,2-c]quinoline-4-one derivatives as novel hedgehog signaling inhibitors. *Bioorg. Med. Chem*. **2012**, *20*, 5496–5506.

35. Matzen, L.; Van Amsterdam, C.; Rautenberg, W.; Greiner, H. E.; Harting, J.; Seyfried, C.A.; Bottcher H. 5-HT reuptake inhibitors with 5-HT1B/1D antagonistic activity: a new approach toward efficient antidepressants. *J. Med. Chem.* **2000**, *43,* 1149–1157.

36. a) Gaglione, M.; Potenza, N.; Di Fabio, G.; Romanucci, V.; Mosca, N.; Russo, A.; Novellino, E.; Cosconati, S.; Messere A. Tuning RNA interference by enhancing siRNA/PAZ recognition. *ACS. Med. Chem. Lett*. **2012**, *4*, 75-78. b) Romanucci, V.; Gaglione, M.; Messere, A.; Potenza, N.; Zarrelli, A.; Noppen, S.; Liekens, S.; Balzarini, J.; Di Fabio, G. Hairpin oligonucleotides forming G-quadruplexes: new aptamers with anti-HIV activity. *Eur. J. Med. Chem.* **2015**, *89*, 51–58.

37. Cantor, C. R.; Warshaw, M. M.; Shapiro, H. Oligonucleotide interactions. III. Circular dichroism studies of the conformation of deoxyoligonucleolides. *Biopolymers* **1970**, *9*, 1059–1077.

38. Pagano, B.; Margarucci, L.; Zizza, P.; Amato, J.; Iaccarino, N.; Cassiano, C.; Salvati, E.; Novellino, E.; Biroccio, A.; Casapullo, A.; Randazzo, A. Identification of novel interactors of human telomeric G-quadruplex DNA. *Chem. Commun.* **2015**, *51*, 2964–2967.

39. Amato, J.; Iaccarino, N.; Pagano, B.; Morigi, R.; Locatelli, A.; Leoni, A.; Rambaldi, M.; Zizza, P.; Biroccio, A.; Novellino, E.; Randazzo, A. Bis-indole derivatives with antitumor activity turn out to be specific ligands of human telomeric G-quadruplex. *Front. Chem.* **2014**, *2*, 54.

40. Scheuermann, T. H.; Padrick, S. B.; Gardner, K. H.; Brautigam. C. A. On the acquisition and analysis of microscale thermophoresis data. *Anal. Biochem.* **2016**, *496*, 79–93.

41. Amato, J.; Morigi, R.; Pagano, B.; Pagano, A.; Ohnmacht, S.; De Magis, A.; Tiang, Y.P.; Capranico, G.; Locatelli, A.; Graziadio, A.; Leoni, A.; Rambaldi, M.; Novellino, E.; Neidle, S.; Randazzo, A. Toward the development of specific G-quadruplex binders: Synthesis, biophysical, and biological studies of new hydrazone derivatives. *J. Med. Chem.* **2016**, *59*, 5706–5720.

42. Brunori, M.; Mathieu, N.; Ricoul, M.; Bauwens, S.; Koering, C. E.; Roborel de Climens, A.; Belleville, A.; Wang, Q.; Puisieux, I.; Décimo, D.; Puisieux, A.; Sabatier, L.; Gilson, E. TRF2 inhibition promotes anchorage independent growth of telomerase-positive human fibroblasts. *Oncogene.* **2006**, *25*, 990–997.

Table of Contents graphic